Tailoring interlayer coupling and coercivity in Co/Mn/Co trilayers by controlling the interface roughness

Bin Zhang, Chii-Bin Wu, and Wolfgang Kuch

Citation: Journal of Applied Physics **115**, 233915 (2014); doi: 10.1063/1.4884235
View online: http://dx.doi.org/10.1063/1.4884235
View Table of Contents: http://scitation.aip.org/content/aip/journal/jap/115/23?ver=pdfcov
Published by the AIP Publishing

Tailoring interlayer coupling and coercivity in Co/Mn/Co trilayers by controlling the interface roughness

Bin Zhang (张彬), Chii-Bin Wu (吴啟彬),[a] and Wolfgang Kuch[b]
Institut für Experimentalphysik, Freie Universität Berlin, Arnimallee 14, 14195 Berlin, Germany

(Received 13 May 2014; accepted 7 June 2014; published online 20 June 2014)

Epitaxial Co/Mn/Co trilayers with a wedged Mn layer were grown on Cu(001) and studied by magneto-optical Kerr effect measurements. The bottom Co film as well as the Mn film exhibits a layer-by-layer growth mode, which allows to modify both interface roughnesses on the atomic scale by tuning the thicknesses of the films to achieve a certain filling of their topmost atomic layers. The onset of antiferromagnetic order in the Mn layer at room temperature was found at thicknesses of 4.1 (4.8) and 3.4 (4.0) atomic monolayers (ML) for a filled (half-filled) topmost atomic layer of the bottom Co film in Mn/Co bilayers and Co/Mn/Co trilayers, respectively. Magnetization loops with only one step were found for a trilayer with half-filled topmost atomic layer of the bottom Co film, while loops with two separate steps have been observed in trilayers with an integer number of atomic layers in the bottom Co film. The coercivity of the top Co film shows an oscillation with 1 ML period as a function of the Mn thickness above 10 ML, which is interpreted as the influence of the atomic-scale control of the interface roughness on the interface exchange coupling between the antiferromagnetic Mn and the top ferromagnetic (FM) Co layer. The strength of the magnetic interlayer coupling between the top and bottom Co layers through the Mn layer for an integer number of atomic layers in the bottom Co layer, deduced from minor-loop measurements, exhibits an oscillation with a period of 2 ML Mn thickness, indicative of direct exchange coupling through the antiferromagnetic Mn layer. In addition, a long-period interlayer coupling of the two FM layers with antiparallel coupling maxima at Mn thicknesses of 2.5, 8.2, and 13.7 ML is observed and attributed to indirect exchange coupling of the Rudermann-Kittel-Kasuya-Yosida type. © *2014 AIP Publishing LLC*. [http://dx.doi.org/10.1063/1.4884235]

I. INTRODUCTION

Magnetic interlayer coupling between two separated ferromagnetic (FM) films across a non-ferromagnetic spacer layer is crucial for many applications in modern magnetic storage devices and spin electronics. If the spacer layer exhibits antiferromagnetic (AFM) order, direct exchange coupling through the spacer layer may contribute to the interlayer coupling, besides the Rudermann-Kittel-Kasuya-Yosida (RKKY)-type interlayer coupling[1–3] and a magnetostatic interaction originating from roughness at the interfaces of the FM layers ("orange peel" coupling) as first pointed out by Néel.[4] Systems containing AFM layers may also exhibit the exchange bias effect.[5,6] Interlayer coupling across AFM spacer layers has been studied and adjusted in several systems. An oscillatory behavior of the coupling in sputtered [Fe/Cr] multilayers corresponding to RKKY-type coupling of 12.5 atomic monolayers (ML) thickness has been reported by Parkin *et al.*[7] In epitaxial [Fe/Cr] multilayers, short-period oscillations with a period of 2–3 ML have been observed,[8] with a large coupling strength due to the direct *d–d* hybridization at the interface. An oscillation of the sign of the interlayer coupling with two-ML periodicity has been reported for an insulating NiO spacer layer in $[Pt/Co]_3$/NiO/$[Pt/Co]_3$ with out-of-plane anisotropy.[9] Zhuravlev *et al.* explained this oscillatory coupling by the interfacial interaction with the uncompensated NiO spins at the interface, which alternates in sign for an odd and even number of monolayers of NiO.[10] Furthermore, a competition between the interlayer and interfacial coupling has been evidenced in Co/(Cr_2O_3, NiO)/Fe trilayers.[11] The interlayer exchange coupling dominates at higher temperatures, while the interfacial exchange interaction exists below the ordering temperature of the AFM layer.

Since the spin direction of AFM materials varies on the length scale of the lattice constant, the exchange coupling between FM and AFM layers depends sensitively on the interface morphology. Single-crystalline systems provide the opportunity to tune the interface roughness on the atomic length scale. In particular, systems that exhibit a layer-by-layer growth allow to modulate the interface roughness by choosing the filling of the terminating atomic layer. The interface coupling of systems with compensated AFM interface spin structure may be enhanced by the controlled incorporation of roughness features. Oscillations of the coercivity H_c and the exchange bias field H_e with a period of 1 ML Co thickness were found in expanded face-centered-tetragonal (e-fct) Mn/Co bilayers on Cu(001), and attributed to the influence of roughness oscillations of the AFM/FM interface due to layer-by-layer growth of the Co layer.[12,13] Atomic-scale control of the AFM–FM exchange coupling was also demonstrated in FeNi/FeMn/Co trilayers.[14]

[a]Present address: Chung Yuan Christian University, 200 Chung Pei Road, Chung Li City, 32023, Taiwan.
[b]E-mail: kuch@physik.fu-berlin.de

We present here a detailed study of tuning the magnetic interlayer coupling in single-crystalline epitaxial Co/e-fct Mn/Co trilayers on Cu(001). Thanks to the layer-by-layer growth of both the bottom Co FM layer as well as the Mn AFM layer, the interface roughness can be selected with atomic precision. We show that in this system, all three interlayer coupling mechanisms, RKKY-type indirect exchange with long-period oscillatory behavior, direct exchange through the AFM layer with an oscillation period of 2 ML of the AFM layer thickness, corresponding to a reversal of the coupling direction with an odd/even number of AFM atomic layers, and magnetostatic Néel-type interlayer coupling, are present. The coercivity of minor loops of the top FM layer exhibits clear oscillations with a periodicity of 1 ML Mn thickness, which can be assigned to roughness oscillations at the upper Co/Mn interface. The maxima of the strength of the interlayer coupling due to direct exchange coupling correlate with the maxima of the coercivity. The interplay of the interlayer coupling together with the exchange bias effect leads to an oscillation of the apparent exchange bias of the top FM layer. Our results demonstrate that the Mn layer thickness as well as the atomic-scale roughnesses of the two interfaces can be used to tailor the magnetic interlayer coupling as well as the coercivities of the FM layers in such FM/AFM/FM trilayers.

Mn is an interesting AFM material because of its rich phase diagram with different ground states corresponding to the α (bcc), β (sc), γ (fcc), and δ (bcc) phases.[15] Even small changes of the axial ratio c/a can induce dramatic changes in the interface coupling. In epitaxial Fe/bct-Mn/Fe (bct: body-centered tetragonal, α phase), the coupling angle between the magnetization directions of the two ferromagnetic Fe layers increases from 0° to 180° and then reduces to 90° with a 2 ML Mn oscillation period.[16] For the [Co/Mn] multilayer case, Kai has calculated that the interlayer exchange coupling both in [Co/α-Mn] and [Co/γ-Mn] multilayers shows oscillations with a period of 2 ML because of the antiferromagnetic order of the Mn layer, while the strength of the interlayer coupling in Co/α-Mn was found weaker than in Co/γ-Mn, which was interpreted as being due to the expanded d-band width and the AFM exchange interaction at the interface.[17] However, no such oscillations with two ML period have been observed in Co/γ-Mn multilayers,[18] and no clear antiferromagnetic coupling between Co layers could be observed in contracted fct Mn/Co multilayers.[19] In Co/Mn/Co on GaAs(001), only one Mn thickness regime with antiferromagnetic interlayer coupling could be observed.[20]

II. EXPERIMENTAL DETAILS

The experiments were performed in an ultrahigh vacuum chamber with a base pressure of $\sim 1 \times 10^{-10}$ mbar. The Cu(001) single crystal of 10 mm diameter with $<0.1°$ miscut was cleaned by cycles of 1 keV Ar^+ ion sputtering and annealing at 830 K for 20 min. Co (Mn) films (Co, Mn rods: 99.99% purity) were deposited at a pressure lower than 2×10^{-10} mbar (4×10^{-10} mbar) by electron-beam-assisted thermal evaporation at room temperature (RT). Typical deposition rates of Co and Mn were 0.5–1 and ~0.3 ML/min, respectively. Uniformity of the film thickness was checked by Auger electron spectroscopy (AES). The Mn layer was prepared as a wedge by moving a shutter in front of the sample. Typical wedge slopes were 0.8–1.4 ML/mm, with a wedge size of 8 mm. Co and Mn thicknesses were calibrated by medium energy electron diffraction (MEED) intensity oscillations during growth and AES. The total error in the thickness calibration of the bottom Co layers is about 0.1 ML. For the Mn wedge, a systematic error of about 10% may be involved in the thickness determination for a certain position along the wedge, while the statistical error is smaller than 0.2 ML. Since the top Co layer does not grow in a layer-by-layer mode, its thickness is determined by the deposition time and the evaporation rate determined by MEED oscillations during the growth of the bottom Co layer. This yields an accuracy of about 10% for the top Co layer thickness.

In-situ magneto-optical Kerr effect (MOKE) measurements were performed in the polar and longitudinal configuration, with a maximum field of 150 mT. A photoelastic modulator and the lock-in technique were used, where the phase of the reflected light was modulated at a retardation of 1/4 of the wavelength. The diode laser (633 nm wavelength) was focused onto the sample with a beam size of around 0.2 mm. The Kerr ellipticity was measured along the [100] azimuth of the sample, and all of the MOKE signals were normalized to the DC intensity at the photodiode detector. All measurements were performed at RT. The bottom Co layer was magnetized in the negative field direction before deposition of the Mn layer. No field cooling procedure was applied.

III. RESULTS AND DISCUSSION

Fig. 1(d) shows typical MEED oscillation curves for the growth of Co on Cu(001) and of Mn on Co/Cu(001). Both

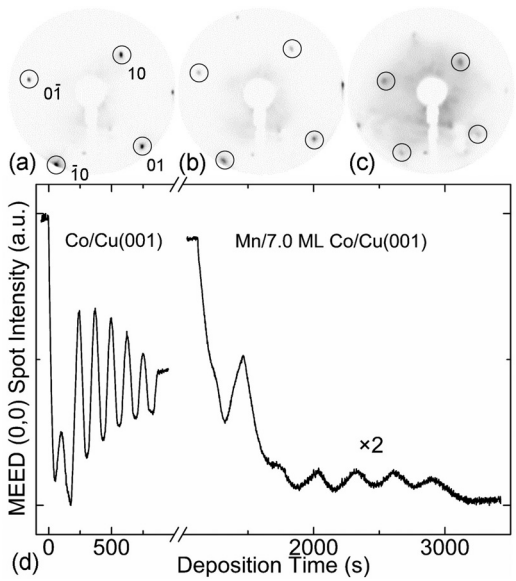

FIG. 1. LEED patterns of (a) Cu(001) (69.8 eV), (b) 10.3 ML Co/Cu(001) (70.2 eV), and (c) 7 ML Mn/10.3 ML Co/Cu(001) (102.6 eV). Black circles indicate the (01) spots. (d) MEED intensity of the (00) spot recorded during the deposition of Co on Cu(001) and Mn on Co/Cu(001) at RT.

show clear periodic oscillations, indicative of layer-by-layer growth. For Mn on Co/Cu(001), the amplitude of the oscillations decreases after the first two monolayers. This can be due to the evolution of the film structure during initial growth of Mn on Co/Cu(001), when Mn atoms fill the channels between Co islands and thus smoothen the surface. Subsequently, this surface forms the substrate for the almost perfect layer-by-layer growth of Mn, which starts from 2 ML thickness.[21,22] Similar MEED curves are also observed for Mn growth on Co films of other thicknesses.[23] Figs. 1(a)–1(c) show low-energy electron diffraction (LEED) patterns of Cu (001), 10.3 ML Co/Cu(001), and 7 ML Mn/10.3 ML Co/Cu (001), respectively. The spot positions are accordant, indicating the coherent growth of Mn/Co on Cu(001). The structure of the Mn lattice in Mn/Co/Cu(001) was determined from LEED-I/V curves (see Fig. S3 of the supplementary material[23]). The simple kinematic analysis of the LEED-I/V curve of the (00) spot of 7 ML Mn/10.3 ML Co/Cu(001) reveals a vertical lattice constant of 1.92 Å, corresponding to an axial ratio $c/a = 1.05 \pm 0.01$. Such an expanded face-centered tetragonal structure of Mn is consistent with theoretical calculations ($c/a = 1.048$ (Ref. 24)) and previous experimental work.[25–27]

In order to study the interface dependence of the interlayer interaction, several bilayer and trilayer (Co/) wedged Mn/Co samples were prepared. First, we compare the results for two different coverages of the bottom Co layer, 10.0 ML and 10.5 ML, which exhibit filled and half-filled topmost atomic layers because of the layer-by-layer growth. These thicknesses represent a good compromise between the amplitude of the MEED oscillations, which are damped for higher Co thicknesses,[23] and the coercive fields, which may become too high for the field range available in our experiments for lower Co thicknesses. Fig. 2 shows normalized magnetic hysteresis loops of bilayer samples, measured by longitudinal MOKE. Square loops with low coercivity (H_c) start from zero Mn thickness; wider loops at around 5 ML Mn thickness are due to the AFM order of Mn. H_c continues to increase with increasing Mn thickness for the bottom Co layer with integer atomic layer filling, whereas it decreases for the bottom Co layer with half-filled termination at Mn thicknesses higher than 5 ML. Since H_c is indicative of the coupling strength of the FM layer to the spin structure of the AFM layer,[28] we conclude that this coupling is stronger for integer atomic layer filling at the interface. All samples with Mn thicknesses above 6–7 ML showed a small exchange bias of <10 mT, however, with a relatively large error (± 2 mT).

Magnetization loops of trilayers with a bottom Co layer thickness of 10.0 ML are presented in Fig. 3. The tilted loop at 2.3 ML Mn thickness indicates antiferromagnetic interlayer coupling. The increase in H_c above 5.1 ML Mn thickness is attributed to the onset of AFM order of Mn. Above 7 ML Mn, loops with two separated steps are observed, where the step with lower coercivity H_s^t corresponds to the top Co layer, the one with higher coercivity H_s^b to the bottom Co layer [Figs. 3(c)–3(d)]. Minor loops were measured in these samples to estimate the size of the interlayer coupling.

The coercivity H_c and the remanent Kerr signal M_r are plotted in Fig. 4 as a function of Mn thickness. The thicknesses of the bottom Co layers were 10.0 ML and 10.5 ML, and the Mn thickness was changed to modulate the interlayer coupling. Let us first look at the data of the Mn/Co bilayer sample [Figs. 4(a) and 4(b)]. For the bottom Co layer of 10.0 ML thickness, there is an initial small decrease of H_c of the bilayer with increasing Mn thickness, hardly visible in Fig. 4(a), which could be due to a change of the interface structure. The bare

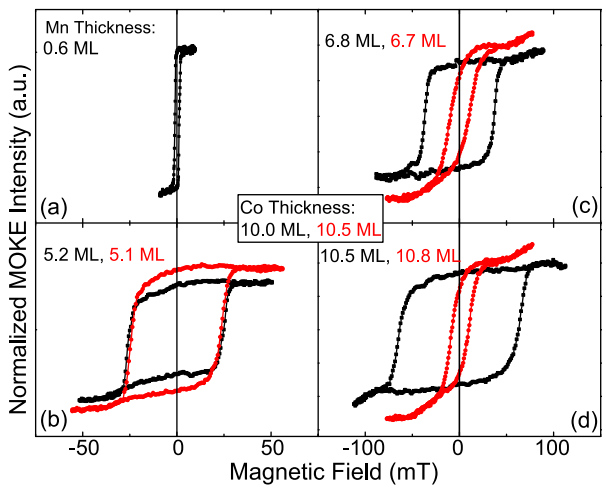

FIG. 2. Hysteresis loops measured with the magnetic field aligned parallel to the in-plane [100] crystal direction for Mn/10.0 ML Co (black) and Mn/10.5 ML Co bilayers (red). The Mn layer thicknesses were (a) 0.6 ML, (b) 6.8 (6.7) ML, (c) 5.2 (5.1) ML, and (d) 10.5 (10.8) ML for 10.0 (10.5) ML bottom Co layer thickness.

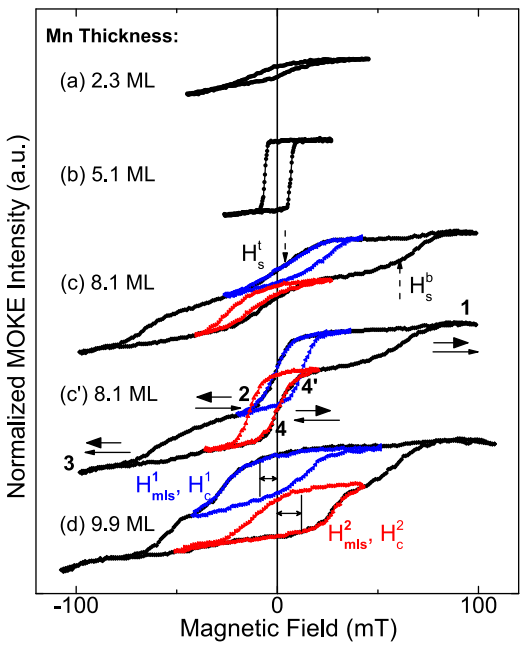

FIG. 3. (a)–(c), (d) Hysteresis loops measured with the magnetic field aligned parallel to the in-plane [100] crystal direction for 10 ML Co/Mn wedge/10.0 ML Co, (c′) for 15 ML Co/Mn wedge/10.0 ML Co. H_s^t and H_s^b label the switching field of the top and the bottom layer, H_c^1 and H_c^2 the coercivity of the top Co layer in the positive and negative field minor loop measurements, respectively. $H^{1,2}_{mls}$ defines the shift of the minor loops with respect to zero field. The arrows in (c′) represent the magnetization of the different layers. The Mn thickness is indicated next to the loops.

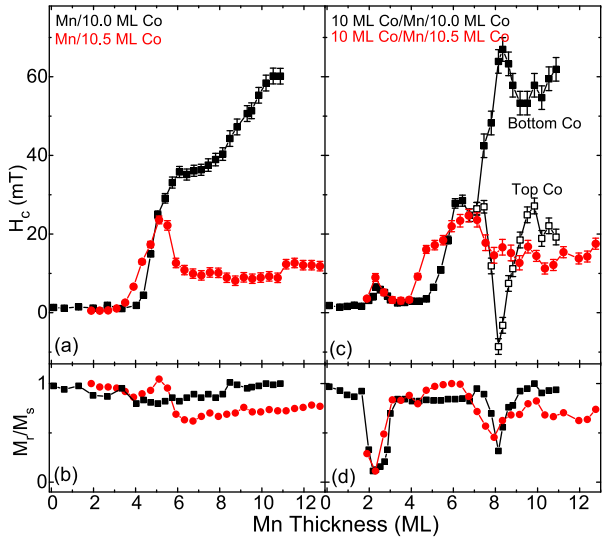

FIG. 4. Top: Coercivity H_c of 0 ML (a) and 10 ML (c) Co/Mn-wedge/Co (bilayer) trilayer sample as a function of Mn thickness. The bottom Co layer thicknesses are 10.0 (black) and 10.5 ML (red), respectively. Above 7 ML Mn two different switching fields (bottom Co layer with higher H_s^b, filled symbols, and top Co layer with lower H_s^t, open symbols) are presented for the trilayer sample with bottom Co layer thickness of 10.0 ML. Bottom: Kerr signal in remanence of the same samples, normalized to saturation.

Co/Cu(001) film reverses mostly by domain nucleation and domain wall (DW) propagation, the additional Mn atoms could increase the nucleation core, and/or reduce the DW depinning field. H_c of the bilayer starts to rise at around 4.1 ML Mn thickness, indicating the onset of AFM order in Mn at RT (t_{AFM}). This thickness is larger than in previous works (2 ML (Ref. 29) and 2.5 ML (Ref. 26)). This difference could arise from the different preparation temperature of Mn (250 K and 330 K, respectively). H_c continues to increase sharply until 6 ML, and then with a slower increase up to around 12 ML, after which it then stays about constant (not shown). Compared to the bilayers with completely filled bottom Co layer, the bilayer samples with bottom Co layer of 10.5 ML show a lower t_{AFM} of around 3.4 ML Mn thickness. The second difference between the two samples that can be related to the different interface roughness is that the H_c of the 10.5 ML bottom Co layer shows a sharp maximum at around 5 ML Mn thickness and then strikingly decreases to less than half the value of this maximum. This behavior is consistent with data of a wedged Mn/20 ML Co/Cu(001) bilayer,[26] and may thus be explained by assuming a similar interface roughness of our 10.5 ML and the 20 ML Co layers in Ref. 26. A dependence of H_c on the AFM/FM interface roughness has been observed before in Mn/Co bilayers, and has been attributed to a biquadratic exchange interaction between FM and AFM spins due to roughness.[12,13]

We now turn to the trilayer systems. First let us see the results for the 10 ML Co/Mn/10.0 ML Co trilayer [black data points in Figs. 4(c) and 4(d)]. Here, both H_c and M_r decrease a bit between 0 and 1.5 ML Mn thickness. The slightly higher coercivity at 0 ML Mn can be attributed to the structural relaxation of the strained Co layer by the appearance of misfit dislocations at the higher total Co thickness when no Mn is present, while with increasing Mn thickness the Co is divided into two separate layers by the Mn spacer layer. As the Mn thickness increases, an unexpected antiparallel interlayer coupling at around 2.5 ML Mn thickness is observed. Tilted loops with large H_c and reduced M_r are observed in that Mn thickness range [Fig. 3(a)]. Even the maximum available field was not sufficient to saturate the sample at this Mn thickness, which indicates that the two FM layers are strongly antiferromagnetically coupled to each other. We cannot exclude that at this thickness (around 2.5 ML Mn) a mixed phase of FM and AFM order exists, similar to what has been concluded for Mn/Co bilayers,[29,30] and also contributes to the antiparallel coupling. Competition between direct exchange and indirect RKKY coupling has been also found in Fe/V(001), where the first AF coupling is missing due to suppression by the V–V direct exchange coupling from the transient ferromagnetism.[31]

From the increase of H_c as a function of Mn thickness, the onset thickness for AFM order of Mn at RT is deduced as 4.8 ML, which is about 0.7 ML (Δt_{AFM}) thicker than in the bilayer. This could be related to proximity effects at the interfaces, which can influence the ordering temperature of an ultrathin AFM layer,[32] or to a change of the effective thickness due to alloying at the interface.[33] A reduced remanence is again observed at around 8.2 ML Mn thickness. Figs. 3(c) and 3(c′) show the major and minor loops at 8.1 ML Mn for 10 and 15 ML Co/Mn/10.0 ML Co, respectively. One notices that the major and minor loops overcross for the 15 ML Co/Mn/10.0 ML Co trilayer [Fig. 3(c′)]. This is because the thicker top Co layer has the lower coercivity and the higher total moment compared to the thinner bottom Co layer. When the major loop is measured for a field sweep from $+H$ [1 in Fig. 3(c′)] to $-H$ [3 in Fig. 3(c′)] and back to $+H$, the top Co layer reverses back into the positive direction at point 4 with a large change in the Kerr signal while the bottom layer still stays magnetized in the negative field direction. For the minor loop, in contrast, a field sweep from $+H$ [1 in Fig. 3(c′)] to $-H_{min}$ [2 in Fig. 3(c′)] and back to $+H$, the bottom Co layer stays magnetized in the positive direction and the top Co layer reverses its magnetization into the positive direction at point 4′, which is at a larger positive field than point 4 of the major loop because of the antiparallel coupling to the bottom layer. The overcrossing occurs because the thicker top Co layer exhibits the larger Kerr signal.

From the shift field H_{mls} of the minor loops of trilayer samples with a bottom Co layer of 10.0 ML (Fig. 3), we can estimate the interlayer coupling energy J using $J = M_s\, d\, \mu_0 (H^2_{mls} - H^1_{mls})/2$, where $M_s = 1440$ kA/m is the saturation magnetization, and $d = 1.7$ and 2.6 nm for 10 ML and 15 ML top Co layer, respectively, is the thickness of the magnetically softer FM layer. We obtain a value of $-33.8\ \mu J/m^2$ for both 15 ML and 10 ML Co top layer samples at 8.1 ML Mn thickness. This confirms that the antiferromagnetic RKKY coupling strength is independent of the FM layer thickness. The coupling strength is nearly the same as in a Co/Cu/Co trilayer (≈ -0.05 mJ/m^2) at the second antiferromagnetic RKKY maximum at 11.5 ML Cu thickness.[34]

Now we compare to the results of the 10 ML Co/Mn/10.5 ML Co trilayer. The first AF coupling is also found at around 2.5 ML Mn thickness. These trilayers show a lower

t_{AFM} (4 ML) and also a smaller difference between the t_{AFM} of the bilayer and the trilayer ($\Delta t_{AFM} = 0.6$ ML). The maximum peak of H_c is at a 1 ML higher Mn thickness than in the bilayer. Finally, a major difference to the case of the atomically filled 10.0 ML bottom Co layer is that magnetization loops with only one step are observed for all Mn thicknesses under study. This could be due to the lower coercivity of the bottom Co layer, as seen from the Mn/10.5 ML Co bilayer. It is more similar to the coercivity of the top Co layer, which could lead to a merging of the magnetization reversals, possibly also mediated by stray fields from propagating domain walls. Furthermore, above 8 ML Mn thickness the H_c of 10 ML Co/Mn/10.5 ML Co shows an oscillation with a period of around 1 ML Mn thickness, which can be attributed to the layer-by-layer growth of Mn on Co. We will discuss this further down in connection with the behavior of the 10 ML Co/Mn/10.0 ML Co trilayers at higher Mn thicknesses.

In order to study in detail the dependence of the magnetic interlayer coupling on the roughness of the upper Co/Mn interface, and, in particular, on the Mn thickness, trilayer samples with 10.0 ML bottom Co layer and thicker Mn wedge were prepared. We focus on the minor loops in those samples. The coercivity and the remanence of the minor loop measurements of the top Co layer are presented in Fig. 5. Both show an oscillation with 1 ML period as a function of the Mn layer thickness. The coercivity reflects the AFM–FM exchange coupling strength. Its oscillation can be explained by the modulation of the atomic-scale interface roughness at the upper Co–Mn interface due to the layer-by-layer growth of Mn on Co [Fig. 1(d)]. The atomic-scale roughness at the interface influences the coupling between the FM and the AFM layer, which manifests itself in the enhancement of the coercivity.[28] Since the minor loops are somewhat tilted and not fully saturated at remanence, their remanence follows the coercivity. We note that the oscillation amplitudes also depend on the thickness of the Mn layer. At 12.5 ML Mn thickness, the amplitude of the H_c oscillation is 12 mT and 4 mT for the 10 ML Co and 15 ML Co/Mn/10.0 ML Co trilayers, respectively. At the same time, the amplitude of the oscillation of the remanence is around 50% and 20% of the saturation value for the 10 ML Co and 15 ML Co/Mn/10.0 ML Co trilayers, respectively.

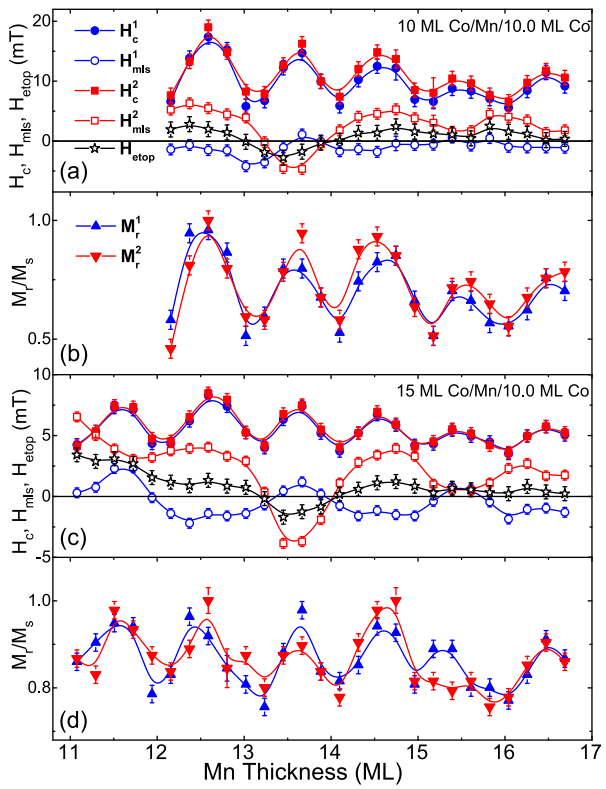

FIG. 5. (a) Coercivity H_c (solid symbols), shift field H_{mls} (open symbols), and (b) M_r of minor loops for a 10 ML Co/Mn wedge/10.0 ML Co and (c) and (d) of a 15 ML Co/Mn wedge/10.0 ML Co trilayer as a function of Mn thickness. H_{etop} (black stars) indicates the exchange bias field of the top Co layer ($H_{etop} = (H^1_{mls} + H^2_{mls})/2$). Solid lines are intended to guide the eye.

The minor loops of the top Co layer also display some horizontal loop shift. This exchange bias of the top FM layer as extracted from the minor loops also seems to oscillate with a 2 ML period (H_{etop} in Fig. 5). However, this might be an artifact induced by the interlayer coupling. The bottom layer exhibits a small negative exchange bias, which manifests itself by a loop shift along the positive field axis, since the Co was saturated along the negative field direction during Mn deposition. Because the two steps from the two Co layers are a bit tilted and not completely separated, and the bottom layer switching fields are not symmetric around zero field due to the exchange bias, the difference between the switching fields of the two steps is smaller in the negative field side than in the positive. When the minor loop H^1 is measured, the top layer reverses when the switching field in the negative direction is reached. If the two loops partly overlap, some part of the bottom layer is also already reversed. So H^1_{mls} becomes larger if there is an antiparallel coupling between the two layers, and becomes smaller if the two layers are coupled parallel to each other. When the minor loop H^2 is measured, the switching fields of the two Co layers are more distinct on the positive field side, and H^2_{mls} is less influenced by the interlayer coupling. So by adding H^1_{mls} and H^2_{mls} to calculate the exchange bias, it will show a positive shift for parallel coupling and a negative shift for antiparallel coupling. This may fully explain why H_{etop} shows the same oscillation as H_{mls}.

The interlayer coupling energy evaluated from H^1_{mls} and H^2_{mls} is plotted in Fig. 6 as a function of Mn thickness. It exhibits an oscillation with a period of 2 ML Mn thickness above a thickness of 10 ML. Such an oscillation may be attributed to direct exchange interaction across the AFM layer. The amplitude of the observed oscillation is about five times smaller compared to the case of Fe/bct-Mn/Fe.[16,35] Another observation is that the oscillation is not around zero, but shifted to the positive side, corresponding to ferromagnetic coupling. This offset of the oscillation points towards an additional Néel-type magnetostatic coupling between the two Co layers.[4] The positive and negative maxima of the coupling strength coincide with the maxima of the coercivity, cf. Fig. 4(a). We conclude that the strength of the interlayer coupling by direct exchange follows the AFM-FM exchange coupling at the interface, which is reflected by the coercivity of the FM layer.

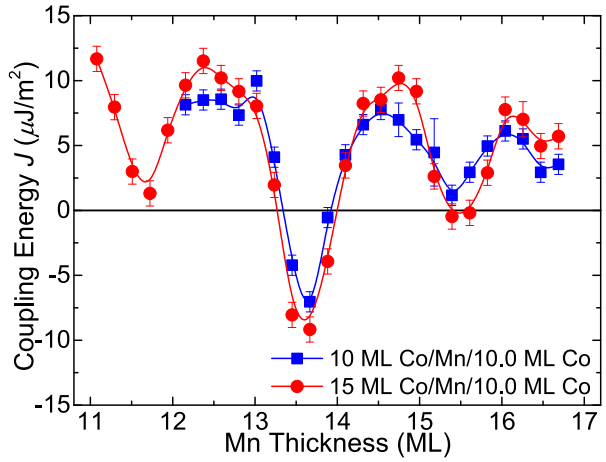

FIG. 6. Interlayer coupling energy extracted from the shift of minor loops as a function of Mn thickness. Solid lines are intended to guide the eye.

The antiferromagnetic coupling around 13.7 ML Mn thickness is probably the superposition of the short-period interlayer coupling by direct exchange and the third antiferromagnetic maximum of the long-period RKKY coupling. We can thus estimate the relative weight of these two contributions to the coupling at this thickness comparing to the adjacent minima in Fig. 6. Both, the direct exchange coupling and the RKKY-type coupling, seem to contribute about equally to the antiferromagnetic coupling ($\approx 10\,\mu J/m^2$ each). This coupling strength is nearly the same as in Co/Cu/Co trilayers at the third antiferromagnetic RKKY maximum at 17 ML Cu thickness.[34] However, the amplitude of the oscillations of the coupling energy with 2 ML period is one order of magnitude smaller compared to the value obtained for about the same spacer layer thickness in Co/FeMn/Co sandwiches.[14] We note that the amplitude of the oscillations is slightly larger for 15 ML top Co layer thickness than in the 10 ML case. This could be either an artifact from an error in the Co thickness determination, or the manifestation of an effective thickness of the top Co layer smaller than the actual thickness.

IV. CONCLUSIONS

We have investigated Co/(e-fct) Mn/Co trilayers on Cu (001) with a wedged Mn layer for integer and half-integer atomic layer filling of the bottom Co layer. We found that trilayer samples, and particularly those with filled atomic layer of the bottom Co layer, show a higher onset thickness of Mn for AFM order at RT compared to Mn/Co bilayer samples. We also found that only one step is observed in magnetization loops of trilayers with half-filled bottom Co layer for all Mn thicknesses up to at least 13 ML, while two separated steps are found at Mn thicknesses above 7 ML in the filled case. We have observed that coercivity and remanence of the top Co layer show an oscillation with 1 ML period as a function of the Mn layer thickness, which we attribute to roughness oscillations at the upper Co–Mn interface induced by the layer-by-layer growth mode of Mn on Co. These observations demonstrate the influence of the interface structure on the magnetism of the Co/Mn/Co systems, and that atomic-scale steps at the interface play an important role in the interlayer interaction and thus for the magnetic properties of the coupled system. The interlayer coupling energy between the two Co layers in the filled bottom Co layer sample exhibits an oscillation with a period of 2 ML Mn thickness in the 0–15 $\mu J/m^2$ range. In addition, a long-range RKKY-type coupling was also observed with a periodicity of ~5.6 ML of Mn thickness. The first AFM coupling maximum observed at unexpectedly low Mn thickness could also be linked to an FM-AFM phase coexistence in the Mn layer. The interplay between direct exchange coupling through the AFM layer, RKKY-type coupling, and Néel-type magnetostatic coupling determines the overall magnetic interlayer coupling in this system. The detailed atomic and magnetic structure at the AFM/FM interface, i.e., lattice mismatch, uncompensated spins, or strain relaxation can also have an influence on the coupling behavior. For applications in nanotechnology, controlling the magnetic properties of coupled systems by atomic-scale manipulation is an interesting possibility. Here, we have shown that it can be used as an independent parameter in addition to the AFM layer thickness to tune the magnetic properties of an FM layer coupled by interlayer coupling to another FM layer.

ACKNOWLEDGMENTS

B. Zhang gratefully acknowledges funding by the China Scholarship Council (2010618020).

[1]M. A. Ruderman and C. Kittel, Phys. Rev. **96**, 99 (1954).
[2]T. Kasuya, Prog. Theor. Phys. **16**, 45 (1956).
[3]K. Yosida, Phys. Rev. **106**, 893 (1957).
[4]L. Néel, C.R. Hebd. Acad. Sci. **255**, 1676 (1962); avaliable at http://gallica.bnf.fr/ark:/12148/bpt6k4003q/f361.image.langEN.
[5]W. H. Meiklejohn and C. P. Bean, Phys. Rev. **102**, 1413 (1956).
[6]J. Nogués and I. K. Schuller, J. Magn. Magn. Mater. **192**, 203 (1999).
[7]S. S. P. Parkin, N. More, and K. P. Roche, Phys. Rev. Lett. **64**, 2304 (1990).
[8]J. Unguris, R. J. Celotta, and D. T. Pierce, Phys. Rev. Lett. **67**, 140 (1991).
[9]Z. Y. Liu and S. Adenwalla, Phys. Rev. Lett. **91**, 037207 (2003).
[10]M. Y. Zhuravlev, E. Y. Tsymbal, and S. S. Jaswal, Phys. Rev. Lett. **92**, 219703 (2004).
[11]X. H. Liu, W. Liu, F. Yang, X. K. Lv, W. B. Cui, S. Guo, W. J. Gong, and Z. D. Zhang, Appl. Phys. Lett. **95**, 222505 (2009).
[12]J. T. Kohlhepp and W. J. M. de Jonge, J. Appl. Phys. **95**, 6840 (2004).
[13]J. T. Kohlhepp, O. Kurnosikov, and W. J. M. de Jonge, J. Magn. Magn. Mater. **286**, 220 (2005).
[14]W. Kuch, L. I. Chelaru, F. Offi, J. Wang, M. Kotsugi, and J. Kirschner, Nature Mater. **5**, 128 (2006).
[15]D. A. Young, *Phase Diagrams of the Elements* (Academic, Berkeley, 1991).
[16]S.-S. Yan, R. Schreiber, F. Voges, C. Osthöver, and P. Grünberg, Phys. Rev. B **59**, R11641 (1999).
[17]T. Kai, J. Magn. Magn. Mater. **214**, 167 (2000).
[18]Y. Henry, V. Pierron-Bohnes, P. Vennégues, and K. Ounadjela, J. Appl. Phys. **76**, 2817 (1994).
[19]Q. Wang, N. Metoki, C. Morawe, T. Zeidler, and H. Zabel, J. Appl. Phys. **78**, 1689 (1995).
[20]Y. Z. Wu, G. S. Dong, and X. F. Jin, Phys. Rev. B **64**, 214406 (2001).
[21]J. T. Kohlhepp, J. Phys. D **40**, 1300 (2007).
[22]J. T. Kohlhepp, H. Wieldraaijer, and W. J. M. de Jonge, J. Mater. Res. **22**, 569 (2007).
[23]See supplementary material at http://dx.doi.org/10.1063/1.4884235 for LEED-IV curves and additional MEED curves.
[24]J. Hafner and D. Spišák, Phys. Rev. B **72**, 144420 (2005).
[25]P. J. Hsu, C. I. Lu, Y. H. Chu, B. Y. Wang, C. B. Wu, L. J. Chen, S. S. Wong, and M. T. Lin, Phys. Rev. B **85**, 174434 (2012).
[26]J. T. Kohlhepp and W. J. M. de Jonge, Phys. Rev. Lett. **96**, 237201 (2006).

[27]C. H. Wang, Y. Y. Huang, and W. C. Lin, J. Appl. Phys. **109**, 103908 (2011).
[28]M. Stampe, P. Stoll, T. Homberg, K. Lenz, and W. Kuch, Phys. Rev. B **81**, 104420 (2010).
[29]M. Caminale, R. Moroni, P. Torelli, W. C. Lin, M. Canepa, L. Mattera, and F. Bisio, Phys. Rev. Lett. **112**, 037201 (2014).
[30]W. L. O'Brien and B. P. Tonner, Phys. Rev. B **50**, 2963 (1994).
[31]G. R. Harp, M. M. Schwickert, M. A. Tomaz, T. Lin, D. Lederman, E. Mayo, and W. L. O'Brien, IEEE Trans. Magn. **34**, 864 (1998).
[32]K. Lenz, S. Zander, and W. Kuch, Phys. Rev. Lett. **98**, 237201 (2007).
[33]M. Erkovan, Y. A. Shokr, D. Schiestl, C. B. Wu, and W. Kuch, "Influence of Ni_xMn_{1-x} thickness and composition on the Curie temperature of Ni in Ni_xMn_{1-x}/Ni bilayers on $Cu_3Au(001)$," J. Magn. Magn. Mater. (published online).
[34]Z. Q. Qiu, J. Pearson, and S. D. Bader, Phys. Rev. B **46**, 8659 (1992).
[35]S. T. Purcell, M. T. Johnson, N. W. E. McGee, R. Coehoorn, and W. Hoving, Phys. Rev. B **45**, 13064 (1992).